AQUA
Water Infrastructure, Ecosystems and Society

IWA PUBLISHING

 AQUA — Water Infrastructure, Ecosystems and Society Vol 72 No 2, 160 doi: 10.2166/aqua.2023.179

Electrochemical detection of nickel(II) and zinc(II) ions by a dicarboxyl-Calix[4]arene-based sensor (Calix/MPA/Au) through differential pulse voltammetry analysis

Siti Fatimah Nur Abdul Aziz[a] and Shahrul Ainliah Alang Ahmad[a,b,*]

[a] Department of Chemistry, Faculty of Science, Universiti Putra Malaysia, Serdang, Selangor 43400, Malaysia
[b] Institute of Nanoscience and Nanotechnology (ION2), Universiti Putra Malaysia, Serdang, Selangor 43400, Malaysia
*Corresponding author. E-mail: ainliah@upm.edu.my

SAA, 0000-0002-5745-5300

ABSTRACT

Herein, we report a facile approach for constructing a calixarene-based electrochemical heavy metal sensor (Calix/MPA/Au) via a one-pot reaction for the detection of Ni(II) and Zn(II) ions. The surface elemental properties and analytical performance of the Calix/MPA/Au sensor were characterized by X-ray photoelectron spectroscopy (XPS) and differential pulse voltammetry (DPV). Under optimum conditions, the sensor exhibited detection limits of 1.5 and 0.34 mg/L at linear ranges of 2.85–6.65 and 0.13–1.68 mg/L for the Zn(II) and Ni(II) ions, respectively. The developed sensor exhibited a better electrochemical performance in the detection of Zn(II) and Ni(II) ions owing to the favourable host–guest interactions between the hydroxyl groups-functionalized lower rim of dicarboxyl-calix[4]arene and the metal ions. The RSD of the five independent Calix/MPA/Au electrode for Zn(II) and Ni(II) ions was calculated to be 16.3 and 16.1%, respectively. Despite the lower sensitivity of the modified electrode towards Ni(II) ions, this finding proves the high selectivity of the calixarene as a detection probe towards the fitted size of guest ion, hence promising to be assembled and explored as a solid-state based-supramolecular host molecule for tracing metal ions.

Key words: calixarene, electrochemical sensor, heavy metal, nickel, zinc

HIGHLIGHTS

- A platform for sensing Zn(II) and Ni(II) ions based on calixarene (Calix[4]/MPA/Au) was developed.
- The detection was investigated using different electrodes; Au, MPA/Au, and Calix[4]/MPA/Au, demonstrating Calix[4]/MPA/Au had the highest current response towards targets due to host–guest interaction.
- The developed sensor exhibited a limit of detection of 1.5 and 0.34 mg/L for Zn(II) and Ni(II) ions, respectively.

GRAPHICAL ABSTRACT

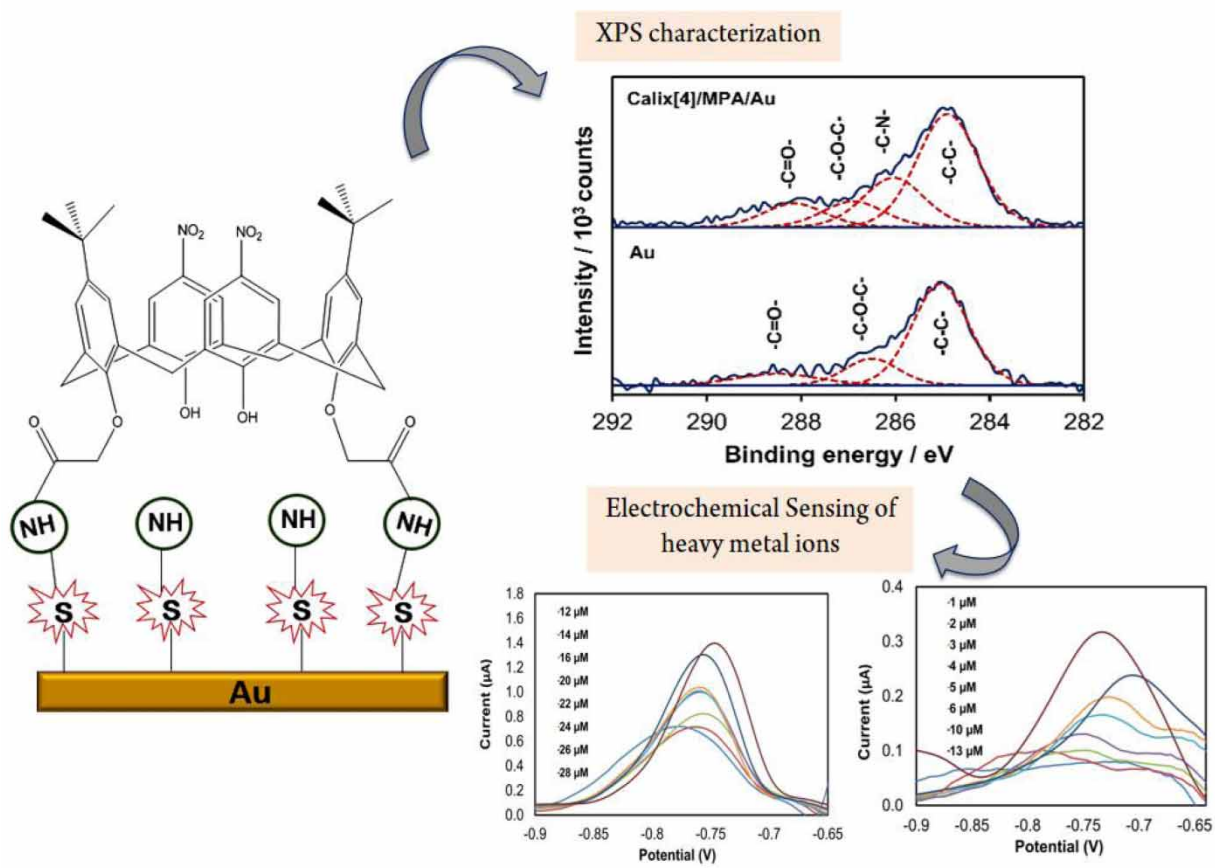

1. INTRODUCTION

Ni(II) and Zn(II) ions, which are naturally found in the Earth's crust, soil, and sediment, pose an environmental and biological risk to the ecosystem when existing in an elevated concentration. According to reports, the corrosion of pipes, water tanks, and pipe coatings is the primary cause of pollution in drinking water sources, notably contamination with metallic elements (ATSDR 2005; Clark *et al.* 2015; World Health Organization 2021). Accredited agencies such as the U.S. Environmental Protection Agency (USEPA) and the World Health Organization (WHO) have established the safe limits for Zn(II) and Ni(II) ion concentrations in water for public drains at 5 and 0.1 mg/L, respectively. Due to their persistence, severe toxicity, and indegradability, heavy metal ions have been categorized as hazardous pollutant agents (Järup 2003; Saha *et al.* 2016). It has been disclosed that excessive exposure to Zn(II) results in complications such as nausea, vomiting, stomach pain, cough, chest pain, dyspnoea, pneumotoria, and acute pnuemonitis due to irritation of the respiratory tract, whereas allergic reaction or dermatitis is the most common adverse effect of Ni(II) exposure (ATSDR 2005; Hannachi *et al.* 2010; Ding *et al.* 2015). In the worst-case scenario, an excess of Zn(II) might cause neurological diseases such as Parkinson's disease, hypoxic ischaemia, and Parkinson's disease and anaemia (Zhou *et al.* 2012). Comparable in toxicity to Zn(II), Ni(II) ion has been found to induce long-term health issues such as respiratory disorders, nasal sinus, lung cancer, and pneumonitis (Patil & Salunke-Gawali 2018).

Conventional analytical techniques for determining the concentration of heavy metal ions include inductively coupled plasma/mass spectrometry (ICP-MS), inductively coupled plasma/atomic emission spectrometry (ICP-AES), atomic absorption spectroscopy (AAS), X-ray fluorescence, ion chromatography, and ultraviolet-visible spectrometry (UV-VIS). Nevertheless, despite their high sensitivity, precision, and versatility in terms of their ability to trace various metal ions, these techniques had several limitations, such as complex analytical processing, time-consuming and tedious sample preparations, costly equipment, the need for trained personnel, and their inapplicability for on-site applications (Dechtrirat

et al. 2018; Eddaif *et al.* 2019; Eddaif *et al.* 2020). In contrast to conventional elemental analysis techniques for tracing heavy metals, electrochemical methods have garnered considerable interest in recent decades as an alternative analytical route due to their relative ease of operation, rapid response, cost-effective fabrication, low-cost instrumentation at high accuracy and precision, and wide linearity of sample concentrations (Afkhami *et al.* 2017; Mei & Ahmad 2021). In addition, other distinctive characteristics of this analysis include the flexibility to miniaturize electrodes and facilitate electrode modification (Kudr *et al.* 2014). Voltammetry is an alternative electrochemical technique that has been extensively employed for the detection of heavy metals in natural water samples because of its excellent stability for *in situ* measurement and quantitative analysis (Afkhami *et al.* 2013). For instance, cyclic, staircase, and pulse are among the most convenient types of approaches used. Differential pulse anodic stripping voltammetry (DPASV) and square wave anodic stripping voltammetry (SWASV) are the most common procedures used to trace heavy metals by using a wide range of working electrodes. Both of these methods have comparable sensitivity but are distinct in the current response measurement. In contrast to the DPV approach, the SWASV method has been demonstrated to be the most sensitive and effective in detecting adsorbed electroactive organic compounds (Lovrić 2010).

The chemical nature of the electrode surface, which relates to the notion of chemically modified electrodes (CME), has a significant impact on the sensitivity of the current response generated by the chosen electrochemical technique. In general, the chemical characteristics and binding properties of a surface electrode are determined by the outermost attached molecule (Murray *et al.* 1987). By altering the surface by irreversible adsorption, it is possible to create self-assembled layers or covalent bonding electrodes with unique features. The modification technique increased the electron transfer kinetics, allowing them to serve as a conducting substrate. Working electrode surfaces such as the carbon paste electrode (CPE), glassy carbon electrode (GCE), and screen-printed electrode (SPE) that have favourable redox behaviour, rapid electron transfer, a broad potential window, and low toxicity are the most common materials that have been modified using the CME technique (Sajid *et al.* 2016). SPEs are of particular interest since they have the potential to be used in mass manufacturing at low cost and could be integrated into portable devices that need just modest sample sizes and minimal reagent usage (Dechtrirat *et al.* 2018). Particularly, the SPCE gold-based construction has garnered attention because of its high electrode transfer, wide anodic potential interval, stability, and chemical reaction resistance (Li & Miao 2013). Gold is the most practical metal surface for SAMs owing to the inclusion of diverse functional groups, which typically results in the production of a well-defined monolayer. In 1983, Nuzzo and Allara were among the pioneering researchers to demonstrate well-directed self-assembly of dialkyl sulphide derivatives on gold surfaces (Bain *et al.* 1989; Wink *et al.* 1997). Due to its resistance to surface alteration, gold substrate appears to be a promising platform for a variety of applications, such as the fabrication of electrochemical sensors.

To maximize the efficiency of electrochemical sensors, selective materials that are employed to build the electrode interfaces have become a key step for the development of high-performance sensors. Calixarene, a macrocyclic chemical first found in 1872 as a byproduct of baeklite synthesis, has sensing applications of interest because of its adaptability in tolerating different kinds of guest ions (Agrawal *et al.* 2010; Vicens & Böhmer 2012; Düker *et al.* 2014). Intrinsically, the variability of host–guest interactions is contributed by the presence of interactions such as ion–dipole, cation–II, anion–II, CH–II, hydrogen bonds, stacking, and van der Waals interactions (Buschmann *et al.* 2001; Udachin *et al.* 2001; Saiapina *et al.* 2016). Calixarene contains an open, rigid, and preorganized scaffold comprised of upper and lower rims that are typically formed via the reaction of p-substituted phenol with formaldehyde. Calixarene may also be modified to have varied sizes and numerous functions, making it a molecule worthy of exploration (Zaghbani *et al.* 2011; Vicens & Böhmer 2012). The functional group attached to the calixarene, such as the phenolic hydroxyl group, contributes to the stability of complex forms by providing a polar environment that is beneficial for zwitterion stability (Arnaud-Neu & Schwing-Weill 1997). Besides, the phenolic hydroxyl groups provide an ideal site for the incorporation of other functional groups including ketone, amide, ester, or carboxylic acid groups, making the calixarene-functionalized hydroxyl group an excellent starting material. Depending on the functional group attached at its rim, the complexity of the compound may vary, increasing in the following sequence: ester < ketone < amide < carboxylic acid (Arnaud-Neu & Schwing-Weill 1997). Published early in 2001 by Honeychurch, two types of calixarene derivatives, which are thiolated 5,11,17,23-tetra-tert-butyl-25,26,27,28-tetrakis-(2-mercaptoethoxy) calix[4] arene and 25,26,27,28-tetrahydroxy-calix[4]arene on screen-printed carbon electrodes, were developed for lead ion detection. This is one of the earlier studies involving the fabrication of a solid-state SPCE sensor using calixarene as the modifier. The LOD was determined to be 5 ng/mL using the DPASV approach. Due to the matrix effect, the performance of the calixarene sensor in real samples was degraded with LOD of 14 ng/mL (Honeychurch *et al.* 2001).

Besides, the outstanding sensing properties of calixarene as a solid-state electrochemical heavy metal-ion sensor can be highlighted from our previous work in which a number of calixarene derivatives were constructed as receptors for detecting metal ions. In the initial study, dicarboethoxy-calix[4]arene was discovered to be selective for single analyte detection, specifically Cu(II), Zn(II), and Fe(II) ions, with detection limits of 9.88 pg/L, 8.33 μg/L, and 1.15 μg/L, respectively (Ruslan *et al.* 2017). Further exploration of the selectivity of calixarene using a different derivative, carboxyl-calix[4]arene, was also reported, and a satisfactory LOD of 6.2 μg/L was observed for the detection of Pb(II) ions in river water samples, with 92% recovery (Nur Abdul Aziz *et al.* 2018). Hence, as part of our ongoing research into calixarene derivatives, we present here the calixarene-derived macrocyclic compound 5,17-dinitro-11,23-di-tert-butyl-25,27-dicarboxy-methoxy-26,28-dihydroxy-calix[4]arene which was fabricated onto a screen-printed gold electrode (Calix/MPA/Au) in the presence of an ethylene diamine linker to detect trace Zn(II) and Ni(II) ions, as shown in Figure 1.

2. MATERIALS AND METHODS

2.1. Chemicals and reagents

All chemicals purchased were of analytical grade and directly used as received. 3-Mercaptopropionic acid (MPA), dimethyl sulphoxide (DMSO) and phosphate-buffered saline (PBS) solution were purchased from Sigma-Aldrich. Potassium chloride (KCl), sulphuric acid, nickel chloride ($NiCl_2$), and copper (II) sulphate ($CuSO_4$) were purchased from R&M chemicals. Ethylene diamine (EDA), 1-ethyl-3-(3-dimethylaminopropyl) carbodiimide (EDC), N-hydroxy succinimide (NHS), and potassium ferricyanide ($K_3[Fe(CN)_6]$) were separately purchased from Acros Organic, Fluka, Alfa Aesar, and Bendosen, respectively. Zinc acetate trihydrate [$Zn(C_2H_3O_2)_2.3H_2O$], lead chloride ($PbCl_2$), and ethanol 97% were purchased from HmbG. All aqueous solutions were prepared in deionized water (18.2 MΩ cm at 25 °C). The dicarboxyl-calix[4]arene used in the experiment was provided by Dr Mary Deasy, a chemist from the Institute of Technology, Tallaght, Dublin, Ireland. Screen-printed gold electrodes (SPGEs)/Ink AT/Work in solution (DRP-C220AT) with dimensions of 3.4 × 1.0 × 0.05 cm (length × width × height) and a working surface dimension of 4 mm were purchased from Metrohm Malaysia Sdn Bhd while a gold electrode with a diameter of 1.6 mm was purchased from BASi, which has been used in a few parameters in the optimization step.

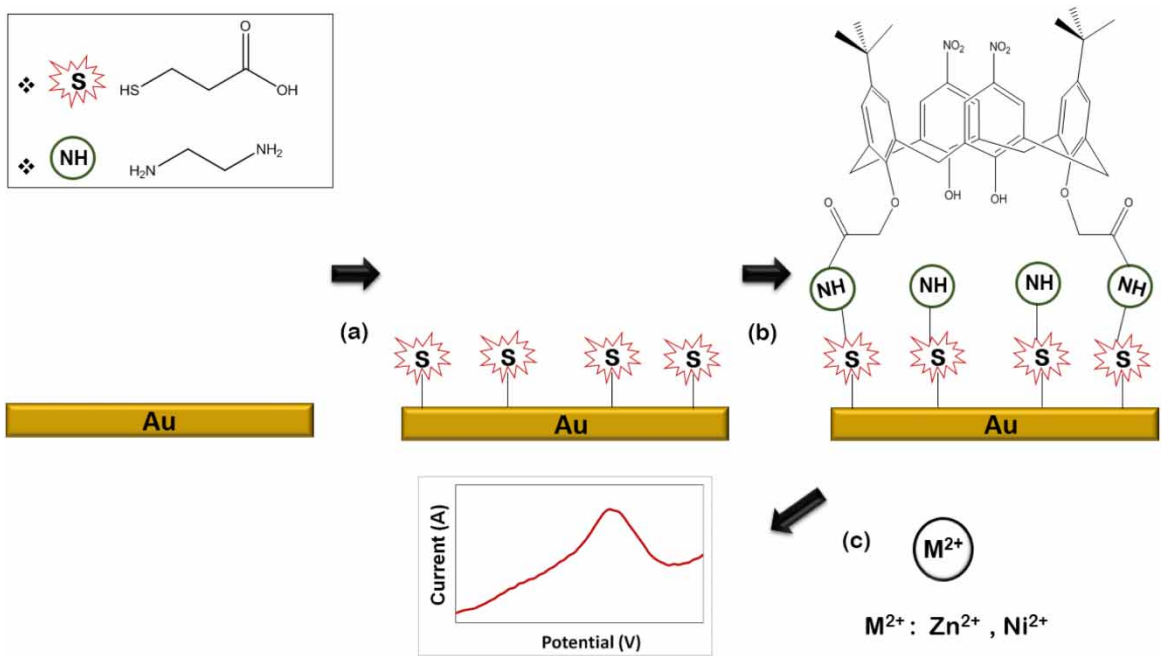

Figure 1 | Schematic representation of the Calix/MPA/Au sensing interface modification for the detection of Zn(II) and Ni(II) ions. (a) Self-assembly of mercaptopropionic acid (MPA) on a gold surface (MPA/Au). (b) Fabrication of the Calix/MPA/Au electrode by a one-pot reaction between EDA, linker 1-ethyl-3-(3-dimethylaminopropyl) carbodiimide (EDC), and N-hydroxy succinimide (NHS) and the modifier, dicarboxyl-calix[4]arene. (c) Detection of Zn(II) and Ni(II) ions using the differential pulse voltammetry (DPV) technique.

2.2. Fabrication of Calix/MPA/Au electrode

The fabrication process of the Calix/MPA/Au electrode was performed in accordance with our previously reported findings (an electrochemical sensing platform for the detection of lead ions based on dicarboxyl-Calix [4] arene). In general, the working gold electrodes were pretreated by immersion in an electrochemical cell containing 0.5 M sulphuric acid solution, followed by 20 cyclic voltammetry (CV) cycle sweeps at a potential window of 0–1.3 V to acquire a clean gold platform. The self-assembly of the MPA monolayer was then performed by dipping the gold surface into 1 mM ethanolic MPA solution, which was then subsequently left in the dark for 24 h. The fabricated electrode (MPA/Au) was immediately used in the next experimental step. The prepared MPA/Au electrode was then fabricated with the dicarboxyl-calix[4]rene modifier. A flowchart depicting the procedure is shown in Figure 1. The carboxyl terminus of MPA/Au was modified by drop-casting a solution of ethylene diamine, EDA (10 mM in DMSO) and dicarboxyl-calix[4]arene (2.0 mg/mL in chloroform) in the presence of EDC/NHS linker (2 mM EDC; 5 mM NHS in DMSO) that had previously been prepared through a one-pot reaction and left for about 1, 2, 3, 4, and 5 h. The Calix/MPA/Au electrode was then dried over a flow of nitrogen and kept at room temperature for detection studies.

2.3. Analytical measurement

The DPV was measured using anodic stripping voltammetry (ASV) mode between –1.2 and 0 V at a scan rate of 100 mV/s, with a conditioning time and equilibrium time of 5 s, followed by a deposition potential at –1.2 V and a deposition time of 120 s.

The electrochemical behaviour of Calix/MPA/Au electrode towards heavy metal ions monolayer was performed through differential pulse voltammetry (DPV) of ASV mode. The modified electrode was immersed in a cell containing 10 mL of 1 μM of analyte in 0.1 M KCl solution. Prior to the DPV measurement, the electrochemical procedure was set to a preconcentration step to enhance the detection signal. The deposition potential was performed at the potential range of –1.3 to –1.0 V for the detection of Ni(II) ion and a potential range of –1.4 to –1.0 V for Zn(II) ion. The parameter was studied in the presence of 1 μM metal analytes in 0.1 M KCl at pH 7 as electrolyte solution for about 120 s. The deposition time of analytes Zn(II) and Ni(II) were varied at five different deposition times; 30, 60, 90, 120, and 150 s employing 0.1 M KCl at pH 7 as supporting medium at the potential of –1.2 V. Following that, the potential was scanned in the range of –1.2 to –0.4 V for Ni(II) ions and –1.3 to – 0.4 V for Zn(II) ion with set deposition potential of –1.2 V for 120 s at a scan rate of 100 mV/s with a conditioning time and equilibrium time of 5 s to acquire a detection peak. All the experiments were conducted at room temperature.

2.4. Instruments

XPS analysis was conducted using an X-ray Microprobe Phi Quantera II with a spectrometer equipped with a monochromated Al Kα scanning X-ray source with an energy of 1,486.6 eV. The wide and high-resolution scans were executed using a beam size of 300 μm with 50 W power and pass energies of 280 and 112 eV, respectively. Prior to elemental analysis, all the binding energies (BEs) were referenced to the carbon C-C component at 285 eV, while the background subtraction was performed with the Casa XPS software using either a linear or Shirley-type method, based on the peak shape fit. The defined peaks were acquired by fitting with the Gauss–Lorentz profile, and the elemental composition data of the electrode surface was displayed. Voltammetric measurements were performed employing an electrochemical system comprised of the AUTOLAB instrument Model uAutolab Type III (Eco Chemie B. V., Netherlands). Reference Ag/AgCl (3.0 M KCl) and counter platinum electrodes were required to run the three-electrode system analysis utilizing the modified gold electrode as the working electrode, whereas a cable connector (CAC) was required for the gold screen-printed electrode (SPE) measurement. The CV and DPV voltammograms were analysed using NOVA 1.11 software.

3. RESULTS AND DISCUSSION

3.1. Surface analysis by X-ray photoelectron spectroscopy

The surface characteristics of the bare Au and Calix/MPA/Au electrodes were determined by XPS analysis. The elemental composition data of the carbon moieties for each surface were analysed on the basis of graphs of intensity against binding energy as depicted in Figure 2(a) and 2(b). The deconvolution of the C1s spectrum of the bare gold surface exhibited chemical shifts at BEs of 285.0, 286.9, and 288.1 eV, attributable to C–C, C–O–C, and C = O, respectively (Bashouti *et al.* 2012; Hsu & Chen 2014). The high intensity of carbon present on a treated gold surface was anticipated as the SPE surface was originally composed of ceramic, carbon, and silver, whereas the presence of oxygen on the surface was due to contamination that

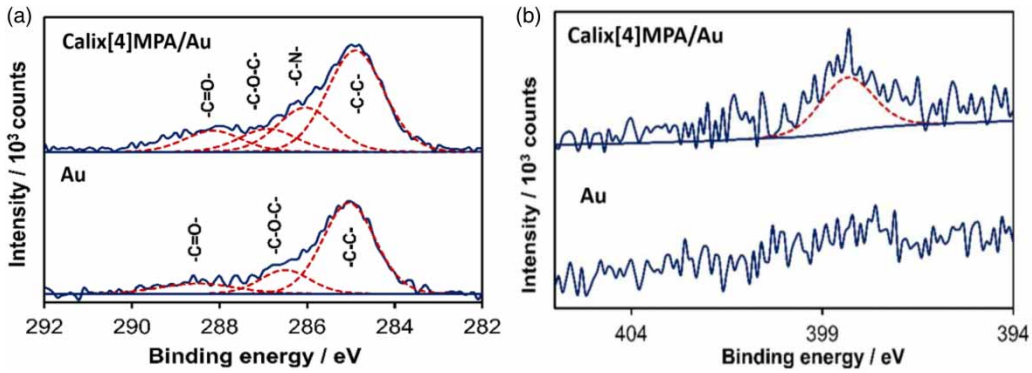

Figure 2 | High-resolution XPS spectra for the (a) C1s spectrum of the Au electrode (bottom) and C1s spectrum of the modified Calix/MPA/Au electrode (top) and (b) N1s spectra of the Au electrode (bottom) and the Calix/MPA/Au electrode (top).

occurred during XPS sample preparation, which involved embedding the solid sample onto the graphite tape, and also, the air exposure allowed a reaction between the hydrocarbons and CO_2 to form carbonates (Korin *et al.* 2017). In comparison with the high-resolution C1s spectrum of the Calix/MPA/Au surface, the emergence of a new peak that was observed at 286.04 eV was ascribed to the C–N bond, suggesting the successful attachment of dicarboxyl-calix[4]arene onto the MPA/Au surface. Figure 2(b) shows the high-resolution scan of the N1s spectra of the bare gold and Calix/MPA/Au surfaces. The photoelectron lines at a binding energy of 398.2 eV were observed in the Calix/MPA/Au spectrum, attributed to the N–H region, and it was expected to have a peak in the binding energy of 406.0 eV, assigned to the nitro group originating from the dicarboxyl-calix[4]arene compound. Nevertheless, due to the X-ray intensity in XPS analysis, the nitro group was likely to reduce to the amine group (El Nahhal *et al.* 2000; Ullien *et al.* 2014). Hence, the disappearance of the peak was observed (Ruslan *et al.* 2017). As for the Au electrode surface, no nitrogen peak was observed.

3.2. Optimization of experimental parameters for Ni(II) and Zn(II) detection

To trace Ni(II) and Zn(II) effectively, the immobilization time of dicarboxyl-calix[4]arene on the working electrode surface, supporting electrolyte, and pH of solution were optimized in an aqueous solution containing 0.1 M KCl utilizing the Calix/MPA/Au electrode. The optimal reaction time required for attaching the modifier onto the electrode surface is crucial as it affects the availability of the binding sites for the analyte species of Ni(II) and Zn(II), which is shown in Figure 3(a). Within a reaction time range of 2–5 h, the highest current signal was measured after 2 h of exposure with dicarboxyl-calixarene, indicating that more active sites, which were cavities in calix[4]arene, were accessible for metal-ion binding. A further increase in the reaction time resulted in a decline of the current response. This phenomenon may be attributable to the use of the bifunctional linker EDA, which formed multilayers via amide linkages with dicarboxyl-calix[4]arene and/or looped structures where both ends of the amine molecules were bound to the surface, consequently creating a sterically hindered effect during the

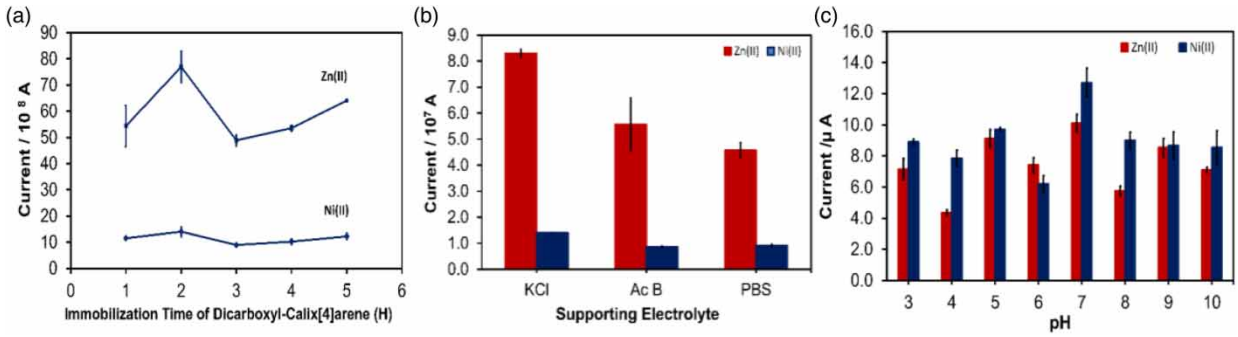

Figure 3 | Effects of (a) immobilization of the modifier, dicarboxyl-calix[4]arene, (b) supporting electrolyte, and (c) pH on the sensitivity of the Calix/MPA/Au sensor towards Zn(II) and Ni(II) ions detection over potential range of –1.2 to –0.4 V and –1.3 to –0.4 V, respectively for 120 s at a scan rate of 100 mV/s.

deposition of dicarboxyl-calixa[4]arene on the surface of the electrode. After 3 h of deposition, the current magnitude starts to increase again due to the less-ordered thickening of the layer as the amine end group that was adsorbed to the surface and the other side became available for amide coupling with the bulky dicarboxyl-calix[4]arene, which offered more binding sites for the metal cations (Wink *et al.* 1997; Huang *et al.* 2014).

Next, the influence of the supporting electrolyte was studied in three types of electrolytes: 0.1 M potassium chloride (pH 5.6), 0.1 M acetate buffer (pH 4.5), and 0.1 M phosphate buffer saline (pH 7) solutions containing 1 μM of metal-ion analyte. Figure 3(b) shows the magnitude of the anodic peak responses of Zn(II) and Ni(II) ions. A high background current was observed in the presence of acetate and phosphate-buffered saline, resulting in the low intensity of the detection peak for both metal ions. Thus, KCl solution was selected as the optimal supporting electrolyte as the highest current magnitude was recorded (Liu *et al.* 2013). Meanwhile, the bar chart illustrated in Figure 3(c) represents the current response of Zn(II) and Ni(II) detection in the pH dependence study. 0.1 M KCl as the supporting electrolyte solution in the pH range of 3.0–10.0 with the presence of a 1 μM metal-ion solution was employed. The pH of the solution was adjusted by adding 0.1 M sodium hydroxide (NaOH) and hydrochloric acid (HCl) solutions to acquire acidic and basic conditions. The results showed that the potential response of the Calix/MPA/Au electrode achieved the best current signal under neutral conditions (pH 7) for both metal ions. At pH < 7, the decrease in current could be ascribed to the partial protonation of the tailored modifier, whereas the formation of hydroxo complexes may have contributed to the decrease in the peak current under more basic conditions (Ganjali *et al.* 2010; Kempegowda & Malingappa 2012; Sharma *et al.* 2013; Huang *et al.* 2014; Liu *et al.* 2015).

3.3. Preconcentration effects on the detection of Ni(II) and Zn(II) ions

Investigating the preconcentration parameters is important to enhance the sensitivity of analyte detection. Generally, the stripping of the preconcentration step will generate the reduction of metal ions and lead to the formation of metal on the working electrode surface. The signal of metal was built during the second stripping, where oxidation of metal that occurred stripped off metal back into solution, producing current and potential readings. Figure 4(a) shows the effect of deposition potential on the metal stripping signals of Zn(II) and Ni(II) ions. When the deposition potential was swept to more negative and positive potentials than –1.3 V, a decrease in current response was observed for Zn(II) detection, implying that the metal ions were reduced completely at more negative potentials (Dong *et al.* 2014). Nonetheless, a reduction in the current signal would be expected in the negative potential region due to the evolution of hydrogen (Barón-Jaimez *et al.* 2013; Rusinek *et al.* 2015; Salih *et al.* 2017). A similar trend was also observed for Ni(II) detection, where the maximum current was achieved at –1.2 V. This was likely because Ni(II) ions required fewer negative potentials to initiate the reduction process than Zn(II) ions based on the Ni(II) standard potential value. The dependence of the DPV stripping current on the deposition times of Zn(II) and Ni(II) ions was further investigated and the results are shown in Figure 4(b). As the deposition time increased, more metal ions were exchanged and adsorbed onto the Calix/MPA/Au electrode surface, resulting in a higher stripping current (Dong *et al.* 2014). The graphs showed that the peak current increased linearly up to 120 s as a longer accumulation time maximized the amounts of Zn(II) and Ni(II) ions that had access to the exposed binding sites of dicarboxyl-calix[4]arene (Liu *et al.* 2015).

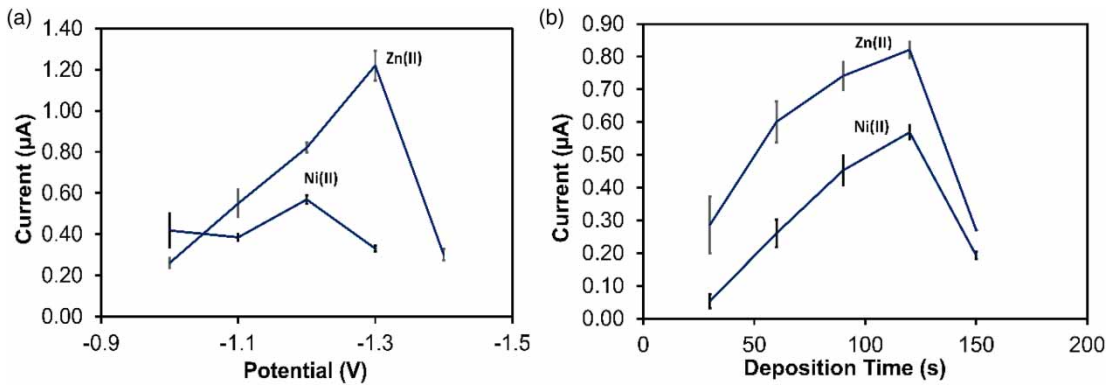

Figure 4 | Effects of (a) deposition potential and (b) deposition time on the voltammetric response of the Calix/MPA/Au sensor for the detection of Zn(II) and Ni(II) ions.

The results suggested that the sensitivity towards the determination of both metal ions increased with time. The curves of current magnitude versus time began to level off when the deposition time exceeded 120 s, indicating that the electrode surface was concentrated with metal analytes. The saturated surface probably affected the electron transfer rate of Zn(II) and Ni(II) stripping (Dong *et al.* 2014).

3.4. Analytical performance of the Calix/MPA/Au electrode towards Zn(II) and Ni(II) ions

Under optimal conditions, the sensitivity of the Calix/MPA/Au electrode towards Zn(II) and Ni(II) ions was determined using DPV. Figure 5(a) depicts the DPV response of the modified electrode to successive additions of Zn(II) at different concentrations in KCl solution at pH 7. A distinguishable anodic peak current was observed, which increased upon increasing the analyte concentration. The Calix/MPA/Au electrode portrayed a linear range for Zn(II) detection up to 28 μM (2.85–6.65 mg/L) with a correlation coefficient of 0.979 and a linearization equation of $I(\mu A) = 0.0427\ x + 0.1539$ as shown in Figure 5(b). The stripping peak potential of Zn(II) appears to be around –0.76 V, with a calculated limit of detection (LOD) of 1.5 mg/L using the formula $3\sigma/s$, where σ is defined as the standard deviation of the blank and s is the slope of the calibration plot. By using a similar experimental design, the Calix/MPA/Au electrode was also utilized to detect Ni(II) in a concentration range of 1–13 μM (0.13–1.68 mg/L) as shown in Figure 5(c). A linear relationship between current magnitude and concentration was observed, with the peak potential of Ni(II) at around –0.74 V. Based on the constructed calibration curve as in Figure 5(d), the regression equation of I (μA) $= 0.0178\ x + 0.0645$ with an R^2 coefficient of 0.9738 was acquired with a detection limit of 0.34 mg/L. The fabricated Calix/MPA/Au electrode also exhibited tolerable sensitivity towards Zn(II) ions, since the LOD reading was slightly below the permissible level at 5.0 mg/L. Nevertheless, based on the

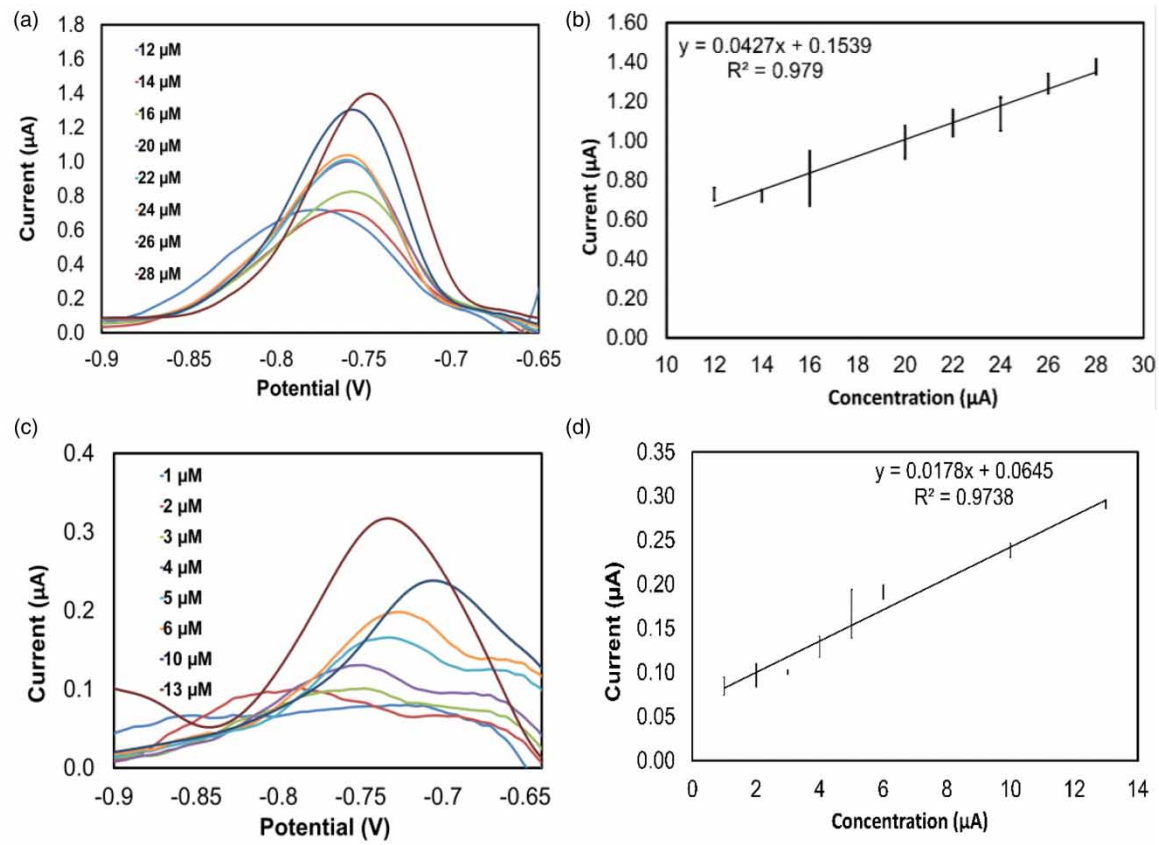

Figure 5 | (a) Anodic peak current response depicting the effect of different Zn(II) concentrations; (b) Calibration curve of the DPV response of Zn(II) at a concentration range of 12–28 μM at a deposition potential of –1.3 V for 120 s with a scan rate of 100 mV/s; (c) DPV stripping peak behaviour of various Ni(II) concentrations in 0.1 M KCl solution; and (d) The calibration curve of the DPV response of Ni(II) at a concentration range of 1–13 μM at a deposition potential of –1.2 V for 120 s with a scan rate of 100 mV/s. The error bar accounts for the relative standard deviation of the two measurements.

computed LOD, the Calix/MPA/Au interface showed poor affinity towards Ni(II) ions, which was higher than the licit threshold level at 0.1 mg/L. This was most likely due to the poor affinity of the hydroxyl groups on the dicarboxyl-calix[4] arene modifier cavity towards Ni(II) ions, resulting in unfavourable interactions between the host and the guest ions.

3.5. Comparative study of Zn(II) and Ni(II) ion detection at the Au, MPA/Au, and Calix/MPA/Au interfaces

To elucidate the effects of different modified interfaces in the detection of Zn(II) and Ni(II) ions, the electrochemical responses of both metal ions were investigated by DPV measurements. The comparative study was performed under optimal conditions with 1 μM concentrations of Zn(II) and Ni(II), and the results are shown in Figure 6(a) and 6(b), respectively. Based on the illustrated bar charts, the Calix/MPA/Au electrode demonstrated an enhancement in current intensity, suggesting that the fabrication process could enhance the interface sensitivity by promoting the migration of redox active analytes to the electrode. Besides, favourable host–guest interactions between the metal ions with oxygen donor atoms of the hydroxyl groups located at the lower rim of dicarboxyl-calix[4]arene could have contributed to the greater current response (Silwa & Girek 2010; Kempegowda & Malingappa 2012). Noticeable current responses of the Au and MPA/Au interfaces towards the detection of Zn(II) and Ni(II) ions were also observed. As reported by Laschi *et al.* in 2006, the recorded detection current by the Au surface was attainable due to the high affinity of Au for the metal ions, whereas the presence of carboxylate anions facilitated electrostatic interactions with the metal ions, which induced the DPV current response (Laschi *et al.* 2006).

3.6. Interference, cycle number, reproducibility, and stability studies of the Calix/MPA/Au electrode

The interference study of the modified Calix/MPA/Au electrode was performed by analysing the DPV responses of Zn(II) and Ni(II) solutions containing possible water-source interferents. The analysis was performed by introducing 1 μM of different bivalent metal ions like Fe(II), Pb(II), Cu(II), Hg(II), Cd(II), and Mg(II) and anions such as Cl^- and SO_4^{2-} individually into KCl solution containing 1 μM of Ni(II) and Zn(II) analytes. Figure 7(a) shows the comparison of the current responses of the control solutions containing 1 μM of Zn(II) and Ni(II) in KCl solution with the current responses of the control solution in the presence of co-existing metal ions of the same concentration. A decrease in peak current of about 61% was recorded in the selectivity study of Ni(II) ions. The current suppression could be attributed to a lack of available dicarboxyl-calix[4]arene active sites to bind to various types of metal ions, as well as the possibility of metal complex formation. Despite the fact that the measurements were conducted in the presence of interferents, Zn(II) selectivity results in an increase in oxidation peak current, which could be ascribed to the presence of metal ions with comparable reduction potentials to Zn(II) ions. The repeatability of the Calix/MPA/Au electrode was evaluated by performing three measurements in the presence of 1 μM Zn(II) and Ni(II) ions under optimized working conditions with a single electrode.

Figure 7(b) depicts the bar chart of Zn(II) and Ni(II) ions current density as a function of DPV cycles. The maximum current was observed in the first DPV measurement cycle. Owing to the fragility of the Calix/MPA/Au electrode, which may have had physical damage, no further treatment was performed to regenerate the modified electrode, thus resulting in the

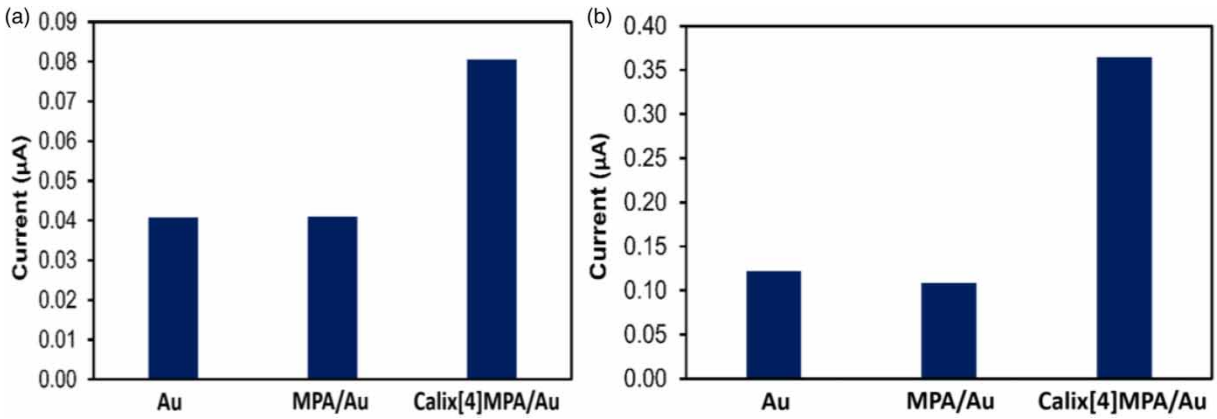

Figure 6 | Current magnitude of each fabricated layer on the gold surface towards the detection of 1 μM (a) Zn(II) and (b) Ni(II) in 0.1 M KCl at pH 7 by DPV measurements in a potential range of −1.2 to −0.4 V at a deposition potential of –1.2 V for 120 s at a scan rate of 100 mV/s.

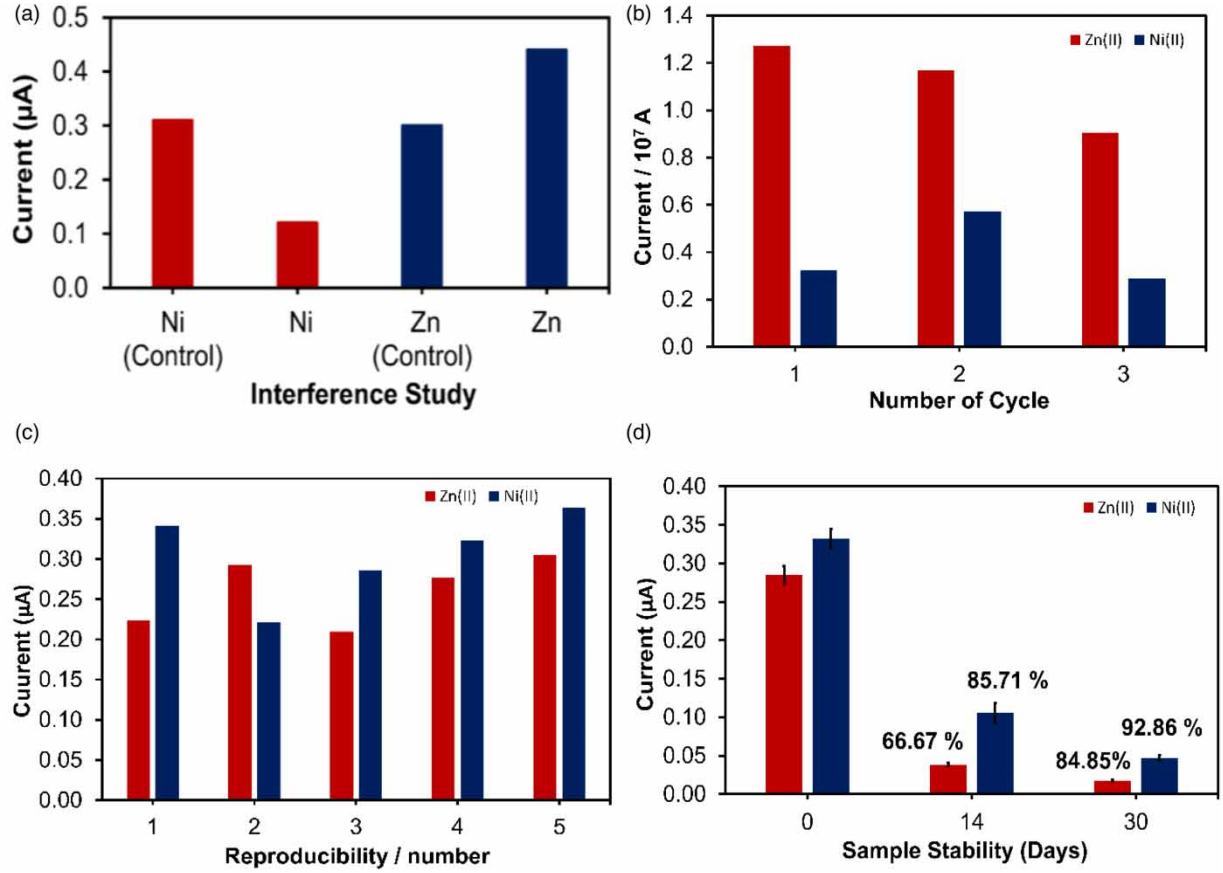

Figure 7 | (a) Representative bar chart of the Calix/MPA/Au sensor's current response on the effect of different metal ions in the control solution (Ni(II)and Zn(II) ions) at the same concentration (1 μM); (b) repeatability, (c) reproducibility, and (d) lifetime studies in 0.1 M KCl solution with the presence of 1 μM Zn(II) and Ni(II) at pH 7 and a scan rate of 100 mV/s.

degradation of sensor performance as more cycles were applied. A further increase in cycle number resulted in the anodic current suppression since there were fewer binding sites accessible on the modified surface due to surface saturation. This demonstrated that the detection of Zn(II) ions by the Calix/MPA/Au electrode was best at the first usage. Meanwhile, a different trend in current response was observed for Ni(II) detection using the Calix/MPA/Au electrode. The anodic current reached its maximum reading on the 2nd cycle, indicating that the modifier on the electrode surface can capture a maximum amount of Ni(II) ions on the second scan. The highest current response was achieved as there were more available sites on the dicarboxyl-calix[4]arene rims that could fit the smaller Ni(II) ions compared with the Zn(II) ions. However, the bulky alkyl group of calix[4]arene was likely to hinder the oxidation and reduction of the captured metal ions in the rims. This explained the current response of Ni(II) ions, which was much smaller than the current response of Zn(II) ions that bound directly to the hydroxyl groups because of their larger size.

The reproducibility of the Calix/MPA/Au electrode was determined on the basis of the RSD values of five independently developed sensors for Zn(II) and Ni(II) cations, which were found to be 16.3 and 16.1%, respectively, as shown in Figure 7(c). The fabrication process involving low concentrations of the bulky modifier (dicarboxyl-calix[4]arene) could have contributed to the high RSD values since the low uniformity of the interface reduced the availability of active sites for metal-ion binding. Moreover, the efficiency of the modified electrode to trace metal ions depended on factors such as the solubility and pH of the prepared solutions, which affected the electroactive species (metal cations) ionic activity present in the solution. The deterioration of the modified electrode surface remains one of the challenges in fabricating electrochemical sensors for industrial purposes. The dependence of the current response on the stability of the Calix/MPA/Au electrode was studied, and readings were obtained periodically after 14 and 30 days. The bar chart in Figure 7(d) illustrates a significant decrease in peak current response up to 92.86% for the Calix/MPA/Au electrode in the presence of Zn(II) ions after a month. A gradual decrease was

also observed during the detection of Ni(II) ions over the same period as the peak was suppressed to 84.85%. The deterioration of the modified electrode stability was ascribable to the degradation of the MPA monolayer, which was first fabricated onto the SPGE surface. This was supported by data obtained from a study done by Mani *et al.* in 2008, who reported that the degradation of the formed thiol derivative monolayer on metal surfaces such as gold and titanium was likely to occur after seven days due to the oxidation process (Mani *et al.* 2008). Thus, a freshly prepared Calix/MPA/Au electrode is recommended to acquire the best sensitivity in the detection of selected metal ions.

4. CONCLUSIONS

In this work, we have successfully incorporated an electrochemical heavy metal-ion sensor for Zn(II) and Ni(II) utilising a screen-printed gold electrode based on calixarene. The macrocyclic molecule whose lower rim was functionalized with a hydroxyl group could well be presented as a potential sensing material that can accommodate metal ions of favourable size via favourable host–guest interaction. The inclusion of calixarene has been demonstrated to enhance the sensitivity for metal-ion detection particularly relative to conductive bare SPGE (Au) and MPA/Au electrodes. The results revealed that the Calix/MPA/Au sensor was considerably sensitive and selective in recognizing Zn(II) ions based on the LOD of 1.5 g/mL in a concentration range of 2.85–6.65 g/mL, which passed the threshold limit. Nevertheless, despite the fact that the modified electrode could only detect Ni(II) concentrations as low as 0.34 g/mL, which is slightly above the permissible limit, the selective properties of the macrocyclic compound in accommodating and forming a complex with the fitted metal ion as a guest ion was still a significant discovery of supramolecular compound as solid-state metal-ion sensor.

ACKNOWLEDGEMENTS

The authors would like to thank the Ministry of Higher Education for financial support via the Fundamental Research Grant Scheme (FRGS/2/2014/ST01/UPM/02/3) and Universiti Putra Malaysia for the Research University Grant Scheme (GP-IPS/2017/9647500) in funding this research project.

AVAILABILITY OF DATA AND MATERIAL

All datasets used in this study are included in the manuscript.

DATA AVAILABILITY STATEMENT

All relevant data are included in the paper or its Supplementary Information.

CONFLICT OF INTEREST

The authors declare there is no conflict.

REFERENCES

Afkhami, A., Bahiraei, A. & Madrakian, T. 2017 Application of nickel zinc ferrite/graphene nanocomposite as a modifier for fabrication of a sensitive electrochemical sensor for determination of omeprazole in real samples. *Journal of Colloid and Interface Science* **495**, 1–8.

Afkhami, A., Soltani-Felehgari, F., Madrakian, T., Ghaedi, H. & Rezaeivala, M. 2013 Fabrication and application of a new modified electrochemical sensor using nano-silica and a newly synthesized Schiff base for simultaneous determination of Cd 2+, Cu 2+ and Hg 2+ ions in water and some foodstuff samples. *Analytica chimica acta* **771**, 21–30.

Agrawal, Y. K., Pancholi, J. P. & Vyas, J. M. 2010 Cheminform abstract: design and synthesis of Calixarene. *ChemInform* **41**, no–no.

Arnaud-Neu, F. & Schwing-Weill, M. J. 1997 Calixarenes, new selective molecular receptors. *Synthetic Metals* **90** (3), 157–164.

ATSDR Agency for Toxic Substances and Disease Registry 2005 *Registry: Toxicological Profile for Nickel*. Available from: https://www.atsdr.cdc.gov/ToxProfiles/tp.asp?id=245&tid=44 (accessed 1 October 2018).

Bain, C. D., Troughton, E. B., Tao, Y. T., Evall, J., Whitesides, G. M. & Nuzzo, R. G. 1989 Formation of monolayer films by the spontaneous assembly of organic thiols from solution onto gold. *Journal of the American Chemical Society* **111** (1), 321–335.

Barón-Jaimez, J., Joya, M. R. & Barba-Ortega, J. 2013 Anodic stripping voltammetry–ASV for determination of heavy metals. In *Journal of Physics: Conference Series*. Vol. 466, No. 1. IOP Publishing, p. 012023.

Bashouti, M. Y., Pietsch, M., Sardashti, K., Brönstrup, G., Schmitt, S. W., Srivastava, S. K., Ristein, J., Arbiol, J., Haick, H. & Christiansen, S. 2012 Hybrid silicon nanowires: from basic research to applied nanotechnology. Nanowires – recent advances, 177–210.

Buschmann, H. J., Mutihac, L. & Jansen, K. 2001 Complexation of some amine compounds by macrocyclic receptors. *Journal of Inclusion Phenomena and Macrocyclic Chemistry* **39** (1), 1–11.

Clark, B. N., Masters, S. V. & Edwards, M. A. 2015 Lead release to drinking water from galvanized steel pipe coatings. *Environmental Engineering Science* **32** (8), 713–721.

Dechtrirat, D., Sookcharoenpinyo, B., Prajongtat, P., Sriprachuabwong, C., Sanguankiat, A., Tuantranont, A. & Hannongbua, S. 2018 An electrochemical MIP sensor for selective detection of salbutamol based on a graphene/PEDOT: PSS modified screen printed carbon electrode. *Rsc Advances* **8** (1), 206–212.

Ding, Y., Zhu, W., Xu, Y. & Qian, X. 2015 A small molecular fluorescent sensor functionalized silica microsphere for detection and removal of mercury, cadmium, and lead ions in aqueous solutions. *Sensors and Actuators B: Chemical* **220**, 762–771.

Dong, Y., Zhou, Y., Ding, Y., Chu, X. & Wang, C. 2014 Sensitive detection of Pb (II) at gold nanoparticle/polyaniline/graphene modified electrode using differential pulse anodic stripping voltammetry. *Analytical Methods* **6** (23), 9367–9374.

Düker, M. H., Kutter, F., Dülcks, T. & Azov, V. A. 2014 Calix [4] arenes with 1, 2-and 1, 3-upper rim tetrathiafulvalene bridges. *Supramolecular Chemistry* **26** (7–8), 552–560.

Eddaif, L., Shaban, A. & Telegdi, J. 2019 Sensitive detection of heavy metals ions based on the calixarene derivatives-modified piezoelectric resonators: a review. *International Journal of Environmental Analytical Chemistry* **99** (9), 824–853.

Eddaif, L., Shaban, A., Telegdi, J. & Szendro, I. 2020 A piezogravimetric sensor platform for sensitive detection of lead (ii) ions in water based on calix [4] resorcinarene macrocycles: synthesis, characterization and detection. *Arabian Journal of Chemistry* **13** (2), 4448–4461.

El Nahhal, I. M., Chehimi, M. M., Cordier, C. & Dodin, G. 2000 XPS, NMR and FTIR structural characterization of polysiloxane-immobilized amine ligand systems. *Journal of Non-Crystalline Solids* **275** (1–2), 142–146.

Ganjali, M. R., Motakef-Kazami, N., Faridbod, F., Khoee, S. & Norouzi, P. 2010 Determination of Pb2 + ions by a modified carbon paste electrode based on multi-walled carbon nanotubes (MWCNTs) and nanosilica. *Journal of Hazardous Materials* **173** (1–3), 415–419.

Hannachi, Y., Shapovalov, N. A. & Hannachi, A. 2010 Adsorption of nickel from aqueous solution by the use of low-cost adsorbents. *Korean Journal of Chemical Engineering* **27** (1), 152–158.

Honeychurch, K. C., Hart, J. P., Cowell, D. C. & Arrigan, D. W. 2001 Voltammetric studies of lead at calixarene modified screen-printed carbon electrodes and its trace determination in water by stripping voltammetry. *Sensors and Actuators B: Chemical* **77** (3), 642–652.

Hsu, K. C. & Chen, D. H. 2014 Microwave-assisted green synthesis of Ag/reduced graphene oxide nanocomposite as a surface-enhanced Raman scattering substrate with high uniformity. *Nanoscale Research Letters* **9** (1), 1–9.

Huang, H., Chen, T., Liu, X. & Ma, H. 2014 Ultrasensitive and simultaneous detection of heavy metal ions based on three-dimensional graphene-carbon nanotubes hybrid electrode materials. *Analytica Chimica Acta* **852**, 45–54.

Järup, L. 2003 Hazards of heavy metal contamination. *British Medical Bulletin* **68** (1), 167–182.

Kempegowda, R. G. & Malingappa, P. 2012 A binderless, covalently bulk modified electrochemical sensor: application to simultaneous determination of lead and cadmium at trace level. *Analytica Chimica Acta* **728**, 9–17.

Korin, E., Froumin, N. & Cohen, S. 2017 Surface analysis of nanocomplexes by X-ray photoelectron spectroscopy (XPS). *ACS Biomaterials Science & Engineering* **3** (6), 882–889.

Kudr, J., Nguyen, H. V., Gumulec, J., Nejdl, L., Blazkova, I., Ruttkay-Nedecky, B., Hynek, D., Kynicky, J., Adam, V. & Kizek, R. 2014 Simultaneous automatic electrochemical detection of zinc, cadmium, copper and lead ions in environmental samples using a thin-film mercury electrode and an artificial neural network. *Sensors* **15** (1), 592–610.

Laschi, S., Palchetti, I. & Mascini, M. 2006 Gold-based screen-printed sensor for detection of trace lead. *Sensors and Actuators B: Chemical* **114** (1), 460–465.

Li, G. & Miao, P. 2013 Theoretical background of electrochemical analysis. In: *Electrochemical Analysis of Proteins and Cells* (Li, G. & Miao, P., eds.). Springer, Berlin, Heidelberg, pp. 5–18.

Liu, L., Wang, C. & Wang, G. 2013 Novel cysteic acid/reduced graphene oxide composite film modified electrode for the selective detection of trace silver ions in natural waters. *Analytical Methods* **5** (20), 5812–5822.

Liu, G., Zhang, Y., Qi, M. & Chen, F. 2015 Covalent anchoring of multifunctionized gold nanoparticles on electrodes towards an electrochemical sensor for the detection of cadmium ions. *Analytical Methods* **7** (13), 5619–5626.

Lovrić, M. 2010 Square-wave voltammetry. In: *Electroanalytical Methods*. (Scholz, F., ed.) Springer, Berlin, Heidelberg, pp. 121–145.

Mani, G., Johnson, D. M., Marton, D., Dougherty, V. L., Feldman, M. D., Patel, D., Ayon, A. A. & Agrawal, C. M. 2008 Stability of self-assembled monolayers on titanium and gold. *Langmuir* **24** (13), 6774–6784.

Mei, C. J. & Ahmad, S. A. A. 2021 A review on the determination heavy metals ions using calixarene-based electrochemical sensors. *Arabian Journal of Chemistry* **14** (9), 103303.

Murray, R. W., Ewing, A. G. & Durst, R. A. 1987 Chemically modified electrodes. Molecular design for electroanalysis. *Analytical Chemistry* **59** (5), 379A–390A.

Nur Abdul Aziz, S. F., Zawawi, R. & Alang Ahmad, S. A. 2018 An electrochemical sensing platform for the detection of lead ions based on dicarboxyl-Calix [4] arene. *Electroanalysis* **30** (3), 533–542.

Patil, A. & Salunke-Gawali, S. 2018 Overview of the chemosensor ligands used for selective detection of anions and metal ions (Zn^{2+}, Cu^{2+}, Ni^{2+}, Co^{2+}, Fe^{2+}, Hg^{2+}). *Inorganica Chimica Acta* **482**, 99–112.

Rusinek, C. A., Bange, A., Papautsky, I. & Heineman, W. R. 2015 Cloud point extraction for electroanalysis: anodic stripping voltammetry of cadmium. *Analytical Chemistry* **87** (12), 6133–6140.

Ruslan, N. I., Lim, D. C. K., Ahmad, S. A., Aziz, S. A., Supian, F. L. & Yusof, N. A. 2017 Ultrasensitive electrochemical detection of metal ions using dicarboethoxycalixarene-based sensor. *Journal of Electroanalytical Chemistry* **799**, 497–504.

Saha, N., Mollah, M. Z. I., Alam, M. F. & Rahman, M. S. 2016 Seasonal investigation of heavy metals in marine fishes captured from the Bay of Bengal and the implications for human health risk assessment. *Food Control* **70**, 110–118.

Saiapina, O. Y., Kharchenko, S. G., Vishnevskii, S. G., Pyeshkova, V. M., Kalchenko, V. I. & Dzyadevych, S. V. 2016 Development of conductometric sensor based on 25, 27-Di-(5-thio-octyloxy) calix [4] arene-crown-6 for determination of ammonium. *Nanoscale Research Letters* **11** (1), 1–10.

Sajid, M., Nazal, M. K., Mansha, M., Alsharaa, A., Jillani, S. M. S. & Basheer, C. 2016 Chemically modified electrodes for electrochemical detection of dopamine in the presence of uric acid and ascorbic acid: a review. *TrAC Trends in Analytical Chemistry* **76**, 15–29.

Salih, F. E., Ouarzane, A. & El Rhazi, M. 2017 Electrochemical detection of lead (II) at bismuth/poly (1, 8-diaminonaphthalene) modified carbon paste electrode. *Arabian Journal of Chemistry* **10** (5), 596–603.

Sharma, R. K., Sharma, S., Gulati, S. & Pandey, A. 2013 Fabrication of a novel nano-composite carbon paste sensor based on silica-nanospheres functionalized with isatin thiosemicarbazone for potentiometric monitoring of Cu^{2+} ions in real samples. *Analytical Methods* **5** (6), 1414–1426.

Silwa, W. & Girek, T. 2010 Calixarene complexes with metal ions. *Journal of Inclusion Phenomena and Macrocyclic Chemistry* **66**, 15–41.

Udachin, K. A., Enright, G. D., Brouwer, E. B. & Ripmeester, J. A. 2001 t-Butylcalix [4] arene compounds with long chain guests: structures and host–guest interactions. *Journal of Supramolecular Chemistry* **1** (2), 97–100.

Ullien, D., Thüne, P. C., Jager, W. F., Sudhölter, E. J. & de Smet, L. C. 2014 Controlled amino-functionalization by electrochemical reduction of bromo and nitro azobenzene layers bound to Si (111) surfaces. *Physical Chemistry Chemical Physics* **16** (36), 19258–19265.

Vicens, J. & Böhmer, V. 2012 *Calixarenes: A Versatile Class of Macrocyclic Compounds*, 1st edn. Springer, Switzerland, AG, p. 264.

Wink, T., Van Zuilen, S. J., Bult, A. & Van Bennekom, W. P. 1997 Self-assembled monolayers for biosensors. *Analyst* **122** (4), 43R–50R.

World Health Organization 2021 *Nickel in Drinking Water: Background Document for Development of WHO Guidelines for Drinking-Water Quality (No. WHO/HEP/ECH/WSH/2021.6)*. World Health Organization, Geneva. Switzerland.

Zaghbani, A., Tayeb, R., Fontas, C., Hidalgo, M., Vocanson, F., Dhahbi, M. & Antico, E. 2011 Thiacalixarene derivatives incorporated in optical-sensing membranes for metal ion recognition. *Analytical Letters* **44** (7), 1241–1253.

Zhou, J. A., Tang, X. L., Cheng, J., Ju, Z. H., Yang, L. Z., Liu, W. S., Chen, C. Y. & Bai, D. C. 2012 An 1, 3, 4-oxadiazole-based OFF–ON fluorescent chemosensor for Zn2+ in aqueous solution and imaging application in living cells. *Dalton Transactions* **41** (35), 10626–10632.

First received 17 October 2022; accepted in revised form 17 January 2023. Available online 2 February 2023